WARSAW UNIVERSITY OF TECHNOLOGY Index 351733
FACULTY OF CIVIL ENGINEERING
COMMITTEE FOR CIVIL AND WATER ENGINEERING
POLISH ACADEMY OF SCIENCES ISSN 1230-2945

DOI: 10.24425/ace.2023.146094

ARCHIVES OF CIVIL ENGINEERING

Vol. LXIX ISSUE 3 2023

 pp. 507 –519

Research paper

The use of genetic expression programming to optimize the parameters of the Muskingum method comparison with numerical methods, Euphrates river a case study

Najah Al-Bedyry[1], Maher Mergan[2], Maha Rasheed[3], Zainab Al-Khafaji[4], Fatimah Nadeem Al-Husseinawi[5]

Abstract: The Muskingham method uses two formulas to describe the translation of flow surges in a river bed. The continuity formula is the first formula, while the relationship between the reach's storage, inflow, and outflow is the second formula (the discharge storage formula); these formulas are applied to a portion of the river between two river cross sections. Several methods can be utilized to estimate the model's parameters. This section contrasts the conventional graphic approach with three numerical methods: Genetic algorithm, Exponential regression, and Classical fourth-order Runge–Kutta. This application's most noticeable plus point was the need to employ a few hydrological variables, such as intake, output, and duration. The location of the Euphrates entrance to the Iraqi territory in Husaybah city was chosen with its hydrological data during the period (1993–2017) to conduct this study. The goal function is established by accuracy criterion approaches (Sum of squares error and sum of squared deviations). Depending on the simulation findings, the suggested predictive flood routing idea was highly acceptable with the prospect of adopting the Genetic Expression Programming model as a suitable and more accurate replacement to existing methods such as the Muskingum model and other numerical models, where this method gave results (R^2 = 0.9984, SSQ = 1.06, SSSD = 80.75), These results achieved a hydrograph that is largely identical to what was given by the hydrological method called Muskingham.

Keywords: river routing, GEP, exponential linear regression, forth-order Runge–Kutta

[1]Ass. Prof., DSc., PhD., Eng., Department of Civil Engineering, College of Engineering / University of Babylon, Babylon, 51001, Iraq, e-mail: eng.najah.kadhim@uobabylon.edu.iq, ORCID: 0000-0002-3186-5248
[2]Ass. Prof., MSc., Eng., Department of Building and Construction Technical, Al-Mussaib Technical College, Al-Furat Al-Awsat Technical University, Babylon, 51006, Iraq, e-mail: maher.mahmood@atu.edu.iq, ORCID: 0000-0001-7130-3373
[3]Ass. Prof., DSc., PhD., Eng., Department of Civil Engineering, College of Engineering / Dijlah University College, Baghdad, 10022, Iraq, e-mail: maha.rasheed@duc.edu.iq, ORCID: 0000-0002-0177-1195
[4]Ass. lecturer., MSc., Eng., Building and Construction Engineering Technology Department, Al-Mustaqbal University College, Hillah 51001, Iraq, ORCID: 0000-0002-5450-7312
[5]Ass. lecturer., MSc., Eng., Al-Turath University College, Baghdad, 10013, Iraq, e-mail: f.civilanna93@gmail.com, ORCID: 0000-0002-6718-361X

1. Introduction

Many methods for forecasting the distinctive features of the movement of a flood wave along a river have been sought after in order to ascertain the steps needed to safeguard people and property from the effects of flooding and to enhance the management of water-related systems along natural or artificial waterways. Many different flow routing models are accurate enough when employed within their constraints to be found in the literature [1–5]. There are two types of flow routing: distributed and lumped. While lumped flow routing, also known as hydrologic routing [6–8], calculates the flow as a time function at a single location along a watercourse, distributed flow routing, also known as hydraulic routing, simultaneously calculates the flow as a time function at numerous cross sections along a river or stream [9, 10]. The numerical Saint-Venant formulas solution is utilized in the majority of distributed routing models; dynamic routing models were essential for slowly rising flood waves in mildly sloping channels (less than 0.10 percent slope), conditions with large backwater effects caused by tides, significant tributary inflows, constrictions, dams, and bridges, and situations where waves propagate upstream from massive tides, storm surges, or extremely significant tributary inflows [11–13]. Because dynamic models can precisely simulate the broadest range of wave types and waterway features, the economic viability of utilizing dynamic routing models for a wider range of applications will steadily increase as the trend of increased computational speed and storage capabilities with decreasing costs continue [14–16]. However, hydrological routing models will continue to be utilized in a range of real-world applications due to their reasonable data requirements and cheap operational costs (such as flood forecasting) [9, 17–19]. The use of genetic algorithms (GA) was made. Genetic operators are often employed in optimization and hydrologic modeling [13, 20–22]. The chosen factors, such as the population size, the number of generations, the types of mutations, selection, crossover, objective magnitude, and the search space constraints, determine how well a GA functions. It is crucial to define the upper and lower boundaries a genetic algorithm searches within [23–26].

The model's parameters of river routing can be determined using a variety of approaches. This artical compares the traditional visual approaches to three numerical methods genetic algorithm, exponential regression, and classical fourth-order Runge–Kutta. This application's most visible advantage was the requirement to use a few hydrologic variables, such as intake, outflow, and time. The Euphrates River was chosen as a case study, and the objective function is determined using accuracy criterion procedures (sum of squared errors and the sum of squared deviations). Based on the simulation results, the proposed predictive flood routing concept was found to be highly acceptable, with the possibility of using the genetic expression programming model as a suitable and more accurate replacement for existing methods such as the Muskingum model and other numerical models.

2. Genetic Expression Technique (GEP)

A genetic programming and genetic algorithm-based algorithm, the GEP, With this technique, linear chromosomes have preset lengths and are computer-coded. The funda-

mental purpose of the GEP is to build a mathematical function from a set of input data. In the GEP procedure, symbolic regression on the mathematical problem is performed utilizing the bulk of the genetic operators from GA. The process starts with a specific number of chromosomes produced for each individual (initial population). Following the expression of these chromosomes, a set of fitness cases is utilized to evaluate each person's fitness. The people are then picked depending on how well they can reproduce through modification [12, 27–29]. Expression trees (ETs) and genomes are the two primary components of the GEP (ETs). One or more genes, each of which is a mathematical formula, may make up a genome. Each gene's mathematical code is expressed in two separate languages known as Karva Language, such as the language of the and the language of the genes. The head and tail of the GEP genes are their two component sections. The head contains variables, constants, and mathematical operators that encrypt mathematical expressions. Variable and constant terminal symbols are found in the tail. More symbols are utilized if the terminal symbols in the head are insufficient to describe a mathematical calculation. The three major GEP operators are cross-over, transposition, and selection (recombination) [30]. These operators change the chromosomes to increase their fitness level for the following generation. The operator rates set at the start of the model creation indicate a particular chance of a chromosome altering. The typical acceptable mutation rate lies between 0.001 and 0.1.

Additionally, 0.1 and 0.4 are suggested magnitudes for the cross-over and transposition operators, respectively. The choice of the fitness function is the first of five significant phases in getting ready to use GEP. For this issue, the phrase that measures the fitness F_i of a specific programmed (i) is as follows:

$$F_i = \sum_{i=1}^{ci} \left[M - C(i,j) - Ti \right] \tag{2.1}$$

where M denotes the selection range, $C(i, j)$ denotes the magnitude returned for fitness case j by the specific chromosome (out of Ct fitness cases), and Tj denotes the desired outcome for fitness case j. The precision is equal to zero, and $F_i = F_{\max} = C_i M$ if $|C(i, j)Tj|$ (the precision) is less than or equal to 0.01. In our instance, we utilized $M = 110$; thus, $f_{\max} = 1100$.

The benefit of this fitness function is that the system may determine its ideal solution. The second significant stage is the selection of the terminals T and functions F utilized to build the chromosomes. The associated factor, i.e., $Q = F_i, T$, makes up the terminal set in this problem. A good approximation may always be made to include all necessary functions, even though selecting the right function set is only sometimes evident [31]. We employed several fundamental mathematical operations $(1/x, x0.5, x0.3, x3, x2)$ and the four fundamental arithmetic operators $(+, -, *, /)$. The selection of the chromosomal architecture, or the size of the head and the number of genes, is the third important phase. Selecting the connection function is the fourth important step. After several tests, it was discovered that the GEP models performed best with a head length of 8, $h = 8$, and three genes per chromosome. Three genes per chromosome and $h = 8$ are the head lengths employed in this investigation. The GEP's sub-ETs (genes) were connected through multiplication. The

set of genetic operators was ultimately comprised of all genetic operators. Table 1 lists the training parameters for the GEP models. The usual statistical measurements determination coefficient R^2 and root-mean-square errors RMSE are utilized to validate the GEP models' performance:

$$R^2 = \left\{ \frac{\sum q_x \, q_y}{\sqrt{\sum q_x^2 \sum q_y^2}} \right\}^2 \tag{2.2}$$

$$\text{RMSE} = \left\{ \frac{\sum \left(q_o - q_p\right)^2}{n} \right\}^{0.5} \tag{2.3}$$

where $q_x = (q_o q_{om})$; $q_y = (q_p q_{pm})$; q_o – detected magnitudes; q_{om} – mean of q_o; q_p – forecast magnitude; q_{pm} – mean of q_p; and n – sample count.

A flowchart for the Genetic Expression Algorithm is demonstrated in Figure 1.

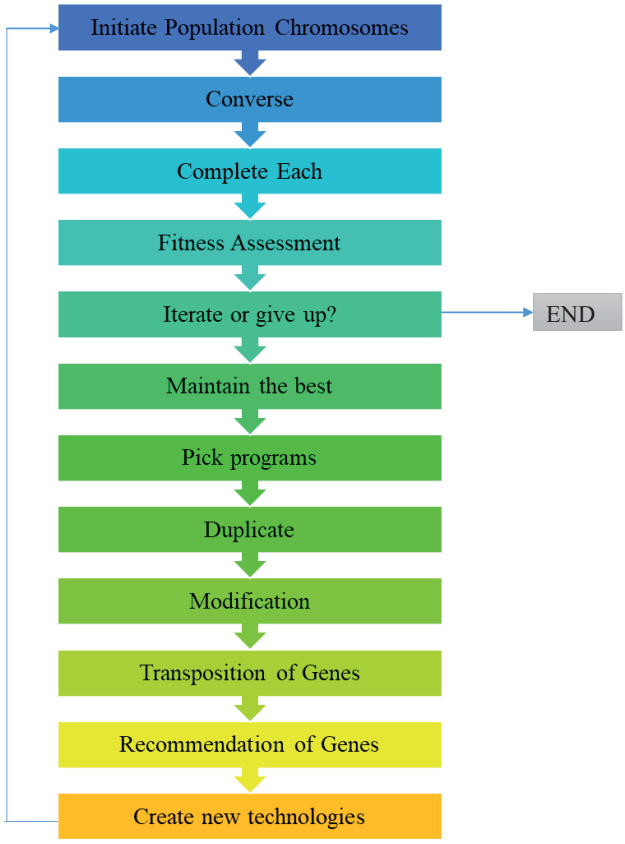

Fig. 1. Genetic Expression Algorithm (GEA) Flowchart

Table 1. Genetic Expression Optimization Parameters

Parameters	Parameters description	Parameters setting
P1	chromosome number	26
P2	type of fitness function mistake	R^2
P3	the number of genes	4
P4	size of the head	12
P5	the linking function	**
P6	set of functions	$+, -, *, /, 1/X, X^{0.5}, X^{0.3}, X^2, X^3$
P7	mutation rate	0.038
P8	rate of one-point recombination	0.35
P9	rate of two-point recombination	0.34
P10	rate of inversion	0.16
P11	rate of transposition	0.17

3. An analytical comparison mechanism

In this study, Muskingham's method was utilized in conjunction with several numerical methods to calculate the parameters of the water storage formula. This decision was made depending on the accuracy and dependability of the findings produced by these methods and the fact that many earlier studies [22, 32] had only sparingly employed them. The selection of a subset of these techniques for this study allowed for analysis, comparison, and an evaluation of the effectiveness of the outcomes.

3.1. Study area

The Euphrates River flows in Turkey, 10 kilometers north of Keban, near the junction of the Murat and Karasu rivers. These rivers have their source in the Armenian uplands, which are over 3000 meters high. Turkey, Syria, and Iraq are all countries through which the Euphrates River primarily runs in a southeasterly direction. The Euphrates and Tigris rivers come together downstream of El-Qurna to form the Shatt-al-Arab River, which flows for 195 kilometers before emptying into the Arabian Gulf; the Euphrates River spans 2210 kilometers from Keban to El-Qurna [32].The location of the Euphrates entrance to the Iraqi territory in Husaybah city was chosen with its hydrological data during the period (1993–2017) to conduct this study.

The main source of river runoff is located in the hilly part of Turkey's Euphrates basin, which has a sophisticated drainage system. The catchment area above Keban town is 64,000 km^2, with an average of 850 mm of precipitation per year. Three important tributaries join the Euphrates on the Syrian desert plateau. The three rivers are the Sadjur River (2,350 km^2), the Balikh River (14,400 km^2), and the Khabur River (36,900 km^2).

While the other two rivers flow below the Tabqa dam, the Sadjur enters the Euphrates above it [4, 33]. At its source near the Syrian-Iraqi border, the Euphrates has historically had an average flow of 870 m^3/s, a maximum flow of 7,400 m^3/s, and a maximum discharge of 13,500 m^3/s with a 0.1% possibility. There are no notable rivers that enter the Euphrates in Iraq.

The river at Haditha, close to the proposed project's site, has a width of 200 to 1100 meters and typical flows of 300 to 7,390 m^3/s. The depth ranges from two to ten meters or more. Speeds are between 0.2 and 3.0 m/sec. The catchment area is 234,600 km^2 above Haditha. About 80 kilometers downstream of Haditha, close to the town of Hit, the river enters the Mesopotamian Plain, the main agricultural region. Three distinct phases can be identified in the river's annual flow:

– Heavy water (flooding) – 70% of the flow is from March to July;
– Low water: 10% of the flow from August to October; and
– High rainfall flows account for 20% of the flow from November to February.

The highest water levels are often seen in April and May, but heavy rains and thawing mountain snow occasionally allow floods to occur in March and even February. The abovementioned data needs to account for the regulatory ramifications of the two dams just finished in Turkey and Syria. The regime of the river has been significantly impacted by these developments, notably during reservoir filling. At this moment, the long-term consequences are unknown. The calculations of Muskingham's approach for the hydrological data of the Euphrates River for the period (1993–2017) indicated in Table 2, Figure 2, demonstrate the catchment area boundaries of the Euphrates river [32].

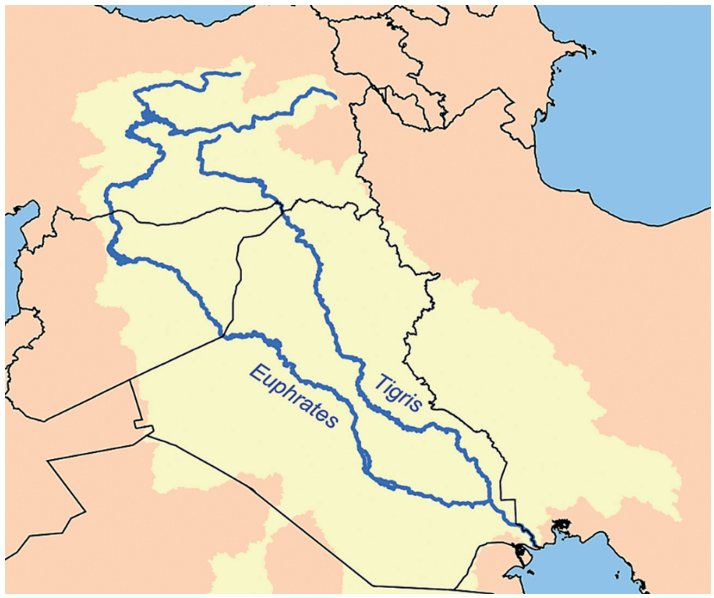

Fig. 2. The Euphrates River's Layout and Catchment Boundaries

Table 2. The monthly average of the inflow and calculated outflow utilizing Muskingham's for the Euphrates River for the period (1993–2017)

Time (hr)	Inflow hydrograph (m^3/s)	Outflow hydrograph (m^3/s)	Time (hr)	Inflow hydrograph (m^3/s)	Outflow hydrograph (m^3/s)
1	95.00	85.00	11	630.0	650.0
2	142.0	95.00	12	575.0	610.0
3	204.0	114.0	13	470.0	615.0
4	322.0	162.0	14	391.0	510.0
5	436.0	230.0	15	325.0	485.0
6	545.0	321.0	16	255.0	400.0
7	623.0	427.0	17	180.0	320.0
8	680.0	500.0	18	130.0	225.0
9	684.0	552.0	19	105.0	200.0
10	672.0	622.0	20	90.00	150.0

4. Numerical approaches

Because several factors influence runoff from precipitation, this method is employed in runoff correlation. The interaction between these two components is extremely intricate. In the case of Muskingum flood guidance, the parameters are calculated depending on the relationship between storage and average wet flow, and the correlation coefficient is determined. Because it was considered in this study that the river basin's catchment area is big [34], it was preferable to employ exponential linear regression, and the general form of this connection is as follows:

$$y = \alpha e^{\beta x} \tag{4.1}$$

by linearizing this exponential form,

$$\ln y = \ln \alpha + \beta x + \varepsilon \tag{4.2}$$

$$y = a + bx + \varepsilon \tag{4.3}$$

in routing form, this formula is:

$$R = aP + b \tag{4.4}$$

where:

$$a = \frac{N\left(\sum PR\right) - \left(\sum P\right)\left(\sum R\right)}{N\left(\sum P^2\right) - \left(\sum P\right)^2} \tag{4.5}$$

$$b = \frac{\sum R - a\left(\sum P\right)}{N}, \quad P = \text{storage } (\text{m}^3) \tag{4.6}$$

$$R = [IX + (1 - X)O]^m \tag{4.7}$$

$$r = \frac{N\left(\sum PR\right) - \left(\sum P\right)\left(\sum R\right)}{\sqrt{\left[\left\{N\left(\sum P^2\right) - \left(\sum P\right)^2\right\} \cdot \left\{N\left(\sum R^2\right) - \left(\sum R\right)^2\right\}\right]}} \tag{4.8}$$

where r = the correlation coefficient.

4.1. Classical forth-order Rung-Kutta method

Utilizing the Muskingum model in its linear form can lead to large errors because the connection between weighted flow and storage is generally nonlinear. In flow direction, the nonlinear Muskingum model is typically utilized, with the following nonlinear storage and continuity formulas:

$$\frac{\mathrm{d}s}{\mathrm{d}t} = I_i - O_i \tag{4.9}$$

$$S_i = K\,[XI_i + (1 - x)O_i]^m \tag{4.10}$$

where: S_i, I_i, and O_i refer to channel storage, inflow, and outflow rate, respectively, at time t. While K, X, and m denote the storage parameter for the river or channel reach, the weighting parameter, and the parameter that accounts for flood wave nonlinearity, respectively. Also, the O and I have similar dimensions to discharge (L^3T^{-1}); and m = dimensionless (–), S has L^3 dimension, and K has $[L^{(1-m)} \cdot T^m]$ dimension. By solving formulas (4.9) and (4.10) for given magnitudes of I_i and parameter magnitudes K, X, and m, the stream flow routing problem decides O_i for any routing time. The outflow is expressed when formula (4.10) is solved for O_i.

$$Q_i = \frac{\left(\frac{si}{k}\right)^{m^{-1}} - xIi}{1 - x} \tag{4.11}$$

The storage volume shift rate concerning time is expressed by substituting O_i from formula (4.11) in formula (4.9).

$$\frac{\mathrm{d}Si}{\mathrm{d}t} = \frac{Ii - \left(\frac{si}{k}\right)^{m^{-1}}}{1 - x} \tag{4.12}$$

Formula (4.12) generates an ordinary first-order differential formula and displays the rate of change in storage, S_i, concerning time t, for given magnitudes of I_i and parameter magnitudes K, m. The beginning magnitude of storage is necessary to solve differential

formula (4.12). The initial outflow is typically believed to be equal to the initial input ($O_o = I_o$); hence, the initial outflow is computed utilizing formula (4.10):

$$S_o = kI_o^m \tag{4.13}$$

$$O_{i+1} = \frac{\left(\frac{S_i + 1}{k}\right)^{m^{-1}} - X\, I_i + 1}{1 - x} \tag{4.14}$$

The steps for employing the Runge–Kutta method of the fourth order are as follows:

1. Assuming the magnitudes of k, x, and m.
2. Determine the initial storage utilizing formula (4.10). S_o, given the magnitudes of I_o and O_o,
3. Determine the quantity of storage that will be required next. S_i is the current magnitude multiplied by the product of the interval volume t and an approximation of the gradient of the next storage evaluation, S_{i+1}. The slope will be computed as a weighted average of the following slopes:

$$K_1 = -\left(\frac{1.0}{1-x}\right)\left(\frac{S_i}{K}\right)^{m^{-1}} + \left(\frac{1.0}{1-x}\right) I_i \tag{4.15}$$

$$K_2 = -\left(\frac{1.0}{1-x}\right)\left(\frac{S_i + 0.5\Delta t K_1}{K}\right)^{m^{-1}} + \left(\frac{1.0}{1-x}\right)\left(\frac{I_i + I_i + 1}{2.0}\right) \tag{4.16}$$

$$K_3 = -\left(\frac{S_i + 0.5\Delta t K_2}{K}\right)^{m^{-1}} + \left(\frac{1.0}{1-x}\right)\left(\frac{I_i + I_i + 1}{2.0}\right) \tag{4.17}$$

$$K_4 = -\left(\frac{S_i + 0.5\Delta t K_3}{K}\right)^{m^{-1}} + \left(\frac{1.0}{1-x}\right) I_{i+1} \tag{4.18}$$

By averaging these four slopes, the following formula can be utilized to compute the next weighted storage:

$$K_{i+1} = S_i + \Delta t\left(\frac{K_1 + 2K_2 + 2K_3 + K_4}{6}\right) \tag{4.19}$$

4. Using formula 10 to calculate the next outflow.
5. Steps 3, 4 should be repeated.

4.2. Methods of accuracy criterion, SSQ, SSSR

The sum of squares error (SSQ) and squared deviations between detected and measured storage rates (SSSR) was utilized to evaluate the outcomes. The discrepancy between the detected magnitude and the projected magnitude is the error. Usually, we wish to reduce the error. The regression is estimating power increases with decreasing error:

$$\text{Minimize(SSQ)} = \sum (O_{ob} - O_{ms})^2 \tag{4.20}$$

$$S_{\text{observed}} = I_i - O_i \tag{4.21}$$

$$S_{\text{computed}} = \frac{d\left[k\left\{XI_i + (1-X)O_i\right\}\right]}{dt} \tag{4.22}$$

The SSSR can be calculated as follows:

$$\text{SSSR} = \sum \left[S_{\text{observed}} - S_{\text{computed}}\right]^2 \tag{4.23}$$

$$\text{SSSR} = \sum_{i=0}^{i=1} \left[\left\{\frac{(I_i + I_i + 1) - (O_i + O_i + 1)}{2}\right\} - \left\{\frac{k\,(x\,I_i + 1 + (1-x)O_i + 1)^m - k\,(xI_i + 1 + (1-x)O_i)}{\Delta t}\right\}\right]^2 \tag{4.24}$$

5. Results analysis and discussion

One of the most important tools for decision-makers and water resource planners to prevent flood tragedies is flood prediction and control. The Muskingum model is one of the most utilized techniques for forecasting flood routes. For precise flood routing, four Muskingum model parameters must be specified. In this case, an optimization process called (GEP) that self-searches for the optimum magnitudes of these parameters may improve the standard Muskingum model. Also, two other numerical approaches were utilized to estimate the outflow. At the beginning of the procedure, the parameters of the evolutionary algorithm have no predetermined magnitudes. As a result, sensitivity analysis was utilized to establish the parameters. For this experiment, the SSQ objective function was employed, and how the objective function magnitude changed for various magnitudes of the parameter was computed. The optimal magnitude for each parameter was selected when the goal function magnitude was lowest. Compared to other approaches, the suggested genetic expression programs depending on the Muskingum model demonstrated good flood routing accuracy while requiring less computational effort, as demonstrated by peak discharge error and time to peak. Given that the inflow and outflow hydrographs display various peak drainage features, the Euphrates river was selected as a good location for the GEP model construction, as demonstrated in Figure 3.

The GEP model led to the optimization of parameters in the Muskingum method, as illustrated in a Table 3. The new GEP technique produces good findings (R^2 = 0.9984)

Table 3. Correlation coefficient R^2 and accuracy criterion, SSQ, SSSR and RMSE

Method	R^2	SSQ	SSSR	RMSE
Muskingham	0.912	2.82	5422.9	1.23
GEP	0.9984	1.06	80.75	1.01
Exponential regression	0.923	2.33	4430.0	1.31
Runge–Kutta	0.90	3.21	5432.6	1.30

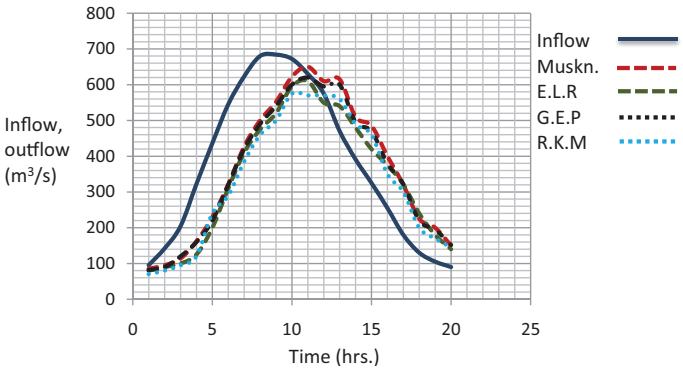

Fig. 3. Flood Hydrograph for study area, Husaybah city

when contrasted with the forecast from the current case study, the SSQ and SSSR for the Muskingum method similar to the rest of the numerical methods, but these values is better for GEP.

6. Conclusions

Depending on the findings of the Euphrates river flood routing investigation, the following conclusions can be made:

1. Depending Muskingum model.
2. Genetic expression model.
3. Exponential regression model.
4. Classical fourth-order Runge–Kutta model.

– Four sets of mathematical modeling of the Euphrates River flood routing were examined on various approaches.
– A very high and positive coefficient of correlation of 0.9984 was obtained from the genetic expression model, along with a standard error of 0.1749. This model produced the curve that fit the field data the best.
– Other researchers could use this novel technique because all the implementation specifics for gene expression programming were properly documented. Additionally, the issues selected to demonstrate how GEP works demonstrate that the new paradigm may be utilized to address a variety of issues from other industries with the benefit of operating effectively on a personal computer.
– The novel idea underlying linear chromosomes and the ETs allowed GEP to perform better than currently utilized adaptive algorithms. As a result, GEP provides new potential for resolving more challenging scientific and technological issues. Another noteworthy and innovative aspect of GEP is its numerous genetic configuration, which turns it into a fully hierarchical discovery method. Finally, since gene expression algorithms more closely mimic nature, they can be utilized to simulate natural evolutionary processes in computers.

References

[1] A.H. Haghiabi, "Estimation of scour downstream of a ski-jump bucket using the multivariate adaptive regression splines", *Scientia Iranica*, vol. 24, no. 4, pp. 1789–1801, 2017, doi: 10.24200/SCI.2017.4270.

[2] B. Knüsel, et al., "Applying big data beyond small problems in climate research", *Nature Climate Change*, vol. 9, no. 3, pp. 196–202, 2019, doi: 10.1038/s41558-019-0404-1.

[3] P. Luo, et al., "Historical assessment of Chinese and Japanese flood management policies and implications for managing future floods", *Environmental Science & Policy*, vol. 48, pp. 265–277, 2015, doi: 10.1016/j.envsci.2014.12.015.

[4] A.I. Requena, F. Chebana, and L. Mediero, "A complete procedure for multivariate index-flood model application", *Journal of Hydrology*, vol. 535, pp. 559–580, 2016, doi: 10.1016/j.jhydrol.2016.02.004.

[5] A. Sharafati, M. Haghbin, D. Motta, and Z.M. Yaseen, "The application of soft computing models and empirical formulations for hydraulic structure scouring depth simulation: a comprehensive review, assessment and possible future research direction", *Archives of Computational Methods in Engineering*, vol. 28, no. 2, pp. 423–447, 2021, doi: 10.1007/s11831-019-09382-4.

[6] I. Iskender and N. Sajikumar, "Evaluation of surface runoff estimation in ungauged watersheds using SWAT and GIUH", *Procedia Technology*, vol. 24, pp. 109–115, 2016, doi: 10.1016/j.protcy.2016.05.016.

[7] A. Kumar, "Geomorphologic instantaneous unit hydrograph based hydrologic response models for ungauged hilly watersheds in India", *Water Resources Management*, vol. 29, no. 3, pp. 863–883, 2015, doi: 10.1007/s11269-014-0848-z.

[8] A. Parsaie, A.H. Haghiabi, M. Saneie, and H. Torabi, "Prediction of energy dissipation of flow over stepped spillways using data-driven models", *Iranian Journal of Science and Technology*, vol. 42, no. 1, pp. 39–53, 2018, doi: 10.1007/s40996-017-0060-5.

[9] M. Najafzadeh, A. Tafarojnoruz, and S.Y. Lim, "Prediction of local scour depth downstream of sluice gates using data-driven models", *ISH Journal of Hydraulic Engineering*, vol. 23, no. 2, pp. 195–202, 2017, doi: 10.1080/09715010.2017.1286614.

[10] A. Pourzangbar, A. Saber, A. Yeganeh-Bakhtiary, and L.R. Ahari, "Predicting scour depth at seawalls using GP and ANNs", *Journal of Hydroinformatics,* vol. 19, no. 3, pp. 349–363, 2017, doi: 10.2166/hydro.2017.125.

[11] K.-S. Cheng, Y.-T. Lien, Y.-C. Wu, and Y.-F. Su, "On the criteria of model performance evaluation for real-time flood forecasting", *Stochastic Environmental Research and Risk Assessment*, vol. 31, no. 5, pp. 1123–1146, 2017, doi: 10.1007/s00477-016-1322-7.

[12] S. Karkheiran, A. Kabiri-Samani, M. Zekri, and H.M. Azamathulla, "Scour at bridge piers in uniform and armored beds under steady and unsteady flow conditions using ANN-APSO and ANN-GA algorithms", *ISH Journal of Hydraulic Engineering*, vol. 27, no. sup1, pp. 220–228, 2021, doi: 10.1080/09715010.2019.1617796.

[13] M. Esmaeili, "Prediction of scour depth around inclined bridge Piers group using optimized ANFIS system parameters with GA", *Journal of Water and Soil Conservation*, vol. 22, no. 6, pp. 283–294, 2016, https://dorl.net/dor/20.1001.1.23222069.1394.22.6.18.0.

[14] M.I. Brunner, D. Viviroli, A.E. Sikorska, O. Vannier, A. Favre, and J. Seibert, "Flood type specific construction of synthetic design hydrographs", *Water Resources Research*, vol. 53, no. 2, pp. 1390–1406, 2017, doi: 10.1002/2016WR019535.

[15] T.J. Wilkinson, L. Rayne, and J. Jotheri, "Hydraulic landscapes in Mesopotamia: The role of human niche construction", *Water History*, vol. 7, no. 4, pp. 397–418, 2015, doi: 10.1007/s12685-015-0127-9.

[16] F. Zaina, "A risk assessment for cultural heritage in southern Iraq: framing drivers, threats and actions affecting archaeological sites", *Conservation and Management of Archaeological Sites*, vol. 21, no. 3, pp. 184–206, 2019, doi: 10.1080/13505033.2019.1662653.

[17] O. Fevzi and O.O. Safak, "Flood routing model using genetic expression programing", in 7*th International Scientific Forum, ISF 2017*. ESI, 2017, pp. 481–490.

[18] E. Plebankiewicz, A. Leśniak, E. Vitkova, and V. Hromadka, "Models for estimating costs of public buildings maintaining-review and assessment", *Archives of Civil Engineering*, vol. 68, no. 1, pp. 335-351, 2022, doi: 10.24425/ace.2022.140171.

[19] A. Dziadosz and A. Kończak, "Review of selected methods of supporting decision-making process in the construction industry", *Archives of Civil Engineering*, vol. 62, no. 1, pp. 111–126, 2016, doi: 10.1515/ace-2015-0055.

[20] M.T. Ayvaz and G. Gurarslan, "A new partitioning approach for nonlinear Muskingum flood routing models with lateral flow contribution", *Journal of Hydrology*, vol. 553, pp. 142–159, 2017, doi: 10.1016/j.jhydrol.2017.07.050.

[21] T. Lillesand, R.W. Kiefer, and J. Chipman, *Remote sensing and image interpretation*. John Wiley & Sons, 2015.

[22] G. Zucco, G. Tayfur, and T. Moramarco, "Reverse flood routing in natural channels using genetic algorithm", *Water Resources Management*, vol. 29, no. 12, pp. 4241–4267, 2015, doi: 10.1007/s11269-015-1058-z.

[23] M.A. Kadhim, N.K. Al-Bedyry, and I.I. Omran, "Evaluation of flood routing models and their relationship to the hydraulic properties of the Diyala River bed", in *IOP Conference Series: Earth and Environmental Science*, vol. 961, no. 1, art. no. 12058, 2022, doi: 10.1088/1755-1315/961/1/012058.

[24] M.A.A. Kadim, I.I. Omran, and A.A.S. Al-Taai, "Optimization of the nonlinear Muskingum model parameters for the river routing, Tigris River a case study", *International Journal of Design & Nature and Ecodynamics*, vol. 16, no. 6, pp. 649–656, 2021, doi: 10.18280/ijdne.160605.

[25] A.R. Vatankhah, "Discussion of 'application of excel solver for parameter estimation of the nonlinear Muskingum models' by Reza Barati", *KSCE Journal of Civil Engineering*, vol. 19, no. 1, pp. 332–336, 2015, doi: 10.1007/s12205-014-1422-1.

[26] M. Chybiński and Ł. Polus, "Experimental and numerical investigations of laminated veneer lumber panels", *Archives of Civil Engineering*, vol. 67, no. 3, pp. 351–372, 2021, doi: 10.24425/ace.2021.138060.

[27] D.J. Armaghani, et al., "On the use of neuro-swarm system to forecast the pile settlement", *Applied Sciences*, vol. 10, no. 6, art. no. 1904, 2020, doi: 10.3390/app10061904.

[28] A.H. Haghiabi, H.M. Azamathulla, and A. Parsaie, "Prediction of head loss on cascade weir using ANN and SVM", *ISH Journal of Hydraulic Engineering*, vol. 23, no. 1, pp. 102–110, 2017, doi: 10.1080/09715010.2016.1241724.

[29] H.-L. Nguyen, et al., "Development of hybrid artificial intelligence approaches and a support vector machine algorithm for predicting the marshall parameters of stone matrix asphalt", *Applied Sciences*, vol. 9, no. 15, art. no. 3172, 2019, doi: 10.3390/app9153172.

[30] A.A. Heidari, S. Mirjalili, H. Faris, I. Aljarah, M. Mafarja, and H. Chen, "Harris hawks optimization: Algorithm and applications", *Future Generation Computer Systems*, vol. 97, pp. 849–872, 2019, doi: 10.1016/j.future.2019.02.028.

[31] A. Malik, A. Kumar, and O. Kisi, "Monthly pan-evaporation estimation in Indian central Himalayas using different heuristic approaches and climate based models", *Computers and Electronics in Agriculture*, vol. 143, pp. 302–313, 2017, doi: 10.1016/j.compag.2017.11.008.

[32] S. Rost, "Water management in Mesopotamia from the sixth till the first millennium BC", *Wiley Interdisciplinary Reviews: Water*, vol. 4, no. 5, art. no. e1230, 2017, doi: 10.1002/wat2.1230.

[33] R. Pappadà, E. Perrone, F. Durante, and G. Salvadori, "Spin-off Extreme Value and Archimedean copulas for estimating the bivariate structural risk", *Stochastic Environmental Research and Risk Assessment*, vol. 30, no. 1, pp. 327–342, 2016, doi: 10.1007/s00477-015-1103-8.

[34] N. Al-Ansari, "Hydro-politics of the Tigris and Euphrates basins", *Engineering*, vol. 8, no. 3, pp. 140–172, 2016, doi: 10.4236/eng.2016.83015.

Received: 2022-11-26, Revised: 2023-04-17